Properties and Structure of the LiCl-films on Lithium Anodes in Liquid Cathodes

Mogensen, Mogens Bjerg; Hennesø, Erik

Published in:
Acta Chimica Slovenica

Link to article, DOI:
10.17344/acsi.2016.2310

Publication date:
2016

Document Version
Publisher's PDF, also known as Version of record

Scientific paper

Properties and Structure of the LiCl-films on Lithium Anodes in Liquid Cathodes

Mogens B. Mogensen and Erik Hennesø

Department of Energy Conversion and Storage, Technical University of Denmark
Frederiksborgvej 399, DK-4000 Roskilde, Denmark

** Corresponding author: E-mail: momo@dtu.dk; erik@hennesoe.com*

Received: 01-02-2016

Dedicated to the memory of Janez Jamnik

Abstract

Lithium anodes passivated by LiCl layers in different types of liquid cathodes (catholytes) based on $LiAlCl_4$ in $SOCl_2$ or SO_2 have been studied by means of impedance spectroscopy. The impedance spectra have been fitted with two equivalent circuits using a nonlinear least squares fit program. Information about the ionic conductivity and the structure of the layers has been extracted. A new physical description, which is able to explain the circuit parameters, is proposed. It assumes that the LiCl-layer contains a large number of narrow tunnels and cracks filled with liquid catholyte. It is explained why such tunnels probably are formed, and for a typical case it is shown that tunnels associated with most of the LiCl grain boundaries of the fine crystalline layer near the Li surface are requested in order to explain the impedance response. The LiCl production rate and through this, the growth rate of the LiCl-layer, is limited by the electron conductivity of the layer. Micro-calorimetry data parallel with impedance spectra are used for determination of the electron conductivity of the LiCl-layer.

Keywords: Lithium batteries, thionyl chloride, solid interphase

1. Introduction

When lithium metal is exposed to an oxidising liquid like $SOCl_2$, a passivating layer of oxidation product, LiCl, will form spontaneously. This layer (which often is called an interphase) and its formation have been extensively investigated in the case of lithium in the $LiAlCl_4$/$SOCl_2$-solution.[1–16] Many different features have been described, and often apparently conflicting data were reported. It is generally accepted, however, that the lithium metal is completely covered by a SEI (= solid electrolyte interphase) consisting of LiCl. The SEI layer forms spontaneously on contact between the lithium and the catholyte. Its thickness is determined by the electron tunnelling range, which, according to Peled is 1.5–2.5 nm.[2] Kazarinov and Bagotzky[11] state that the thickness is 1–1.5 nm directly after contact with the catholyte and growing to 5 nm within the first hours thereafter. These numbers seem to be in fair agreement with general quantum mechanical considerations.[17] The thickness is then increased further with time because electrons can tunnel to energetically favourable defect sites within the film such as dislocations and impurities.[17]

Furthermore, the prevailing view seems to be that on top of the compact primary layer, a porous secondary LiCl layer is formed in a later stage, but other views, different from the prevailing one, have been published as discussed below.[7,12,13,14,15]

Several models of the electrical and/or the microstructural characteristics of the passivating layer have been reported.[1,2,6,7,13,14,16] Most have been of a qualitative descriptive nature, and even though some mathematical formulations have been attempted, e.g. by presuming that the SEI-resistivity is position dependent,[16] no rigorous treatment of the Li-$SOCl_2$-interphase, which was tested extensively against experimental data, has been reported.

The aim of this work is to provide basic information about ionic and electronic conductivity plus structure of the LiCl layers. The electronic conductivity of the layer is derived from parallel measurements of impedance spectra and micro-calorimetry on the same anodes. Further, a dee-

per understanding of the measured impedance spectra of LiCl-interphases has been attempted.

Often, the liquids $LiAlCl_4/SOCl_2$ or $LiAlCl_4/SO_2$ are referred to as the electrolyte. This may be confusing because the solid LiCl-layer in fact is the electrolyte in these cells. Therefore, in the following the term »catholyte« is used for the liquid solutions. The term »electrolyte« is used for the solid LiCl-layer only.

2. Experimental

2. 1. Cell Geometries

Several cell configurations were used. One type of cell had two lithium electrodes in a glass container; size R14 with Teflon lid (Fig. 1). The areas of the lithium electrodes were 23.4 and 9.8 cm², respectively. In the zero polarisation situation this is with respect to impedance equivalent to one electrode having an area of 6.9 cm².

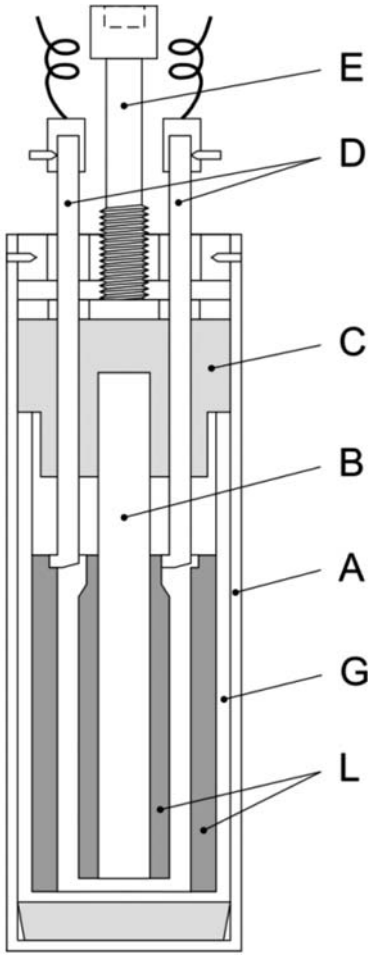

Figure 1. Sketch of the cell with two Li-electrodes (L) in a glass container (G). The cell is assembled in a steel cylinder (A). B is a glass tube supporting the inner Li-electrode, C is a Teflon lid, D points out the SS electrode terminals, and E is a screw which keeps the Teflon lid pressed onto the glass container.

Other types of cells used were 3-electrode cells in glass or in stainless steel (SS) containers, which have been described earlier.[18] The Li reference electrode consists of a 5 mm wide and 1 mm thick Li strip, which was placed vertical between the two current bearing electrodes. The SS-cells included test of measures, which might decrease the passivation rate: (i) adding 1 cm^3 of pure $SOCl_2$ before introducing the catholyte, (ii) adding LiCl-grains to the separator, (iii) pressing a Ni-grid into the Li-surface, and (iv) pressing Ni-fibres into the Li-surface. Electrochemical impedance spectroscopy (EIS) was performed on these cells in order to get input to the understanding of the passivating layers from a variety of Li-anode passivation conditions.

In addition, commercial R14-cells of bobbin type (NIFE) have been measured, which, after 2.5 years, have been regenerated by discharge at 1 Ohm in 15 minutes corresponding to 0.10 Ah = 2% of the total capacity.

Results from all cell types were qualitative in agreement with the description of the LiCl solid electrolyte given below, but only some selected results from the cells listed in Table 1 are reported here.

2. 2. Catholytes

Three types of catholytes were studied: 1) The standard catholyte, which in the following is called the A-catholyte, is thionyl chloride with 1.72 molar $LiAlCl_4$. Its specific ionic conductivity was calculated to be 0.020 S/cm using the formula given by Berg et al.[19] 2) A more acid catholyte, thionyl chloride with 1.2 molar $LiAlCl_4$ and 0.6 molar $AlCl_3SO_2$, is called the B-catholyte. It was originally introduced by Gabano[20] by adding Li_2O to $SOCl_2$ which by reaction form SO_2 and LiCl. Here, however, it was manufactured by adding SO_2 directly instead of Li_2O. 3) Finally, a catholyte consisting of $LiAlCl_4$ and SO_2 only was investigated. It is referred to as the SO_2-catholyte. Gaseous

Table 1. Overview of the cell data. The area of the Li (working) electrodes varies between 20 and 27 cm^2. The exact value is given where needed.

Cell code	Electrodes, container material	Catholyte type	Other characteristics
G40A	3 Li, glass	A	
3201	2 Li, glass	A	
G24 B	3 Li, glass	B	
SO21	3 Li, glass	SO_2	SO_2/Li = 2
3303	2 Li, glass	SO_2	SO_2/Li = 4
602	1 Li + 1 carbon, SS	A	Commercial cell
607	1 Li + 1 carbon, SS	A	Pure $SOCl_2$ added
610	1 Li + 1 carbon, SS	A	LiCl nuclei added
614	1 Li + 1 carbon, SS	A	Ni-grid on anode
618	1 Li + 1 carbon, SS	A	Ni-fibres on anode
2REG	1 Li + 1 carbon, SS	A	Regen. comm. cell

SO_2 was allowed to react with a mixture of $AlCl_3$ and LiCl at 0.5 atm. overpressure overnight, finishing to equilibrium at room temperature at 0.1 atm. overpressure. This gives a liquid molar ratio of Li/SO_2 = 3.2. The ionic conductivity is 0.10 S/cm.[21] Lower Li/SO_2 was prepared by controlling the weight during SO_2 addition.

Table 1 gives an overview of the cells referred to in this paper.

2. 3. Measurement Equipment

The impedance spectra of the cells were measured by a Solatron 1250 Frequency Response Analyzer. The current necessary for the measurements is sufficiently low so that a potentiostat may not be needed. The frequency generator was in this case connected to the cell in series with a capacitor, which was put next to the counter electrode and outside the potential sensing leads, in order to avoid any DC current (i.e. to avoid DC-discharge). In some cases a Solatron 1286 potentiostat was used for the connection to the cells. Measurements were made using a maximum of 2 μA/cm^2 amplitude in the range of 0.1 or 1 Hz to 60 kHz. All measurements were performed at ambient temperature.

The microcalorimeter, which was designed and constructed in-house, is sketched in Fig. 2. In order to facilitate calibration, a 100 kΩ resistor was built into each of the measuring blocks so that a known heat effect can be added e.g. 10 V giving 1 mW. In the calibration mode, an aluminium cylinder which has the same heat capacity as the battery cell is inserted.

During the calorimetric measurements impedance measurements were performed with regular time intervals.

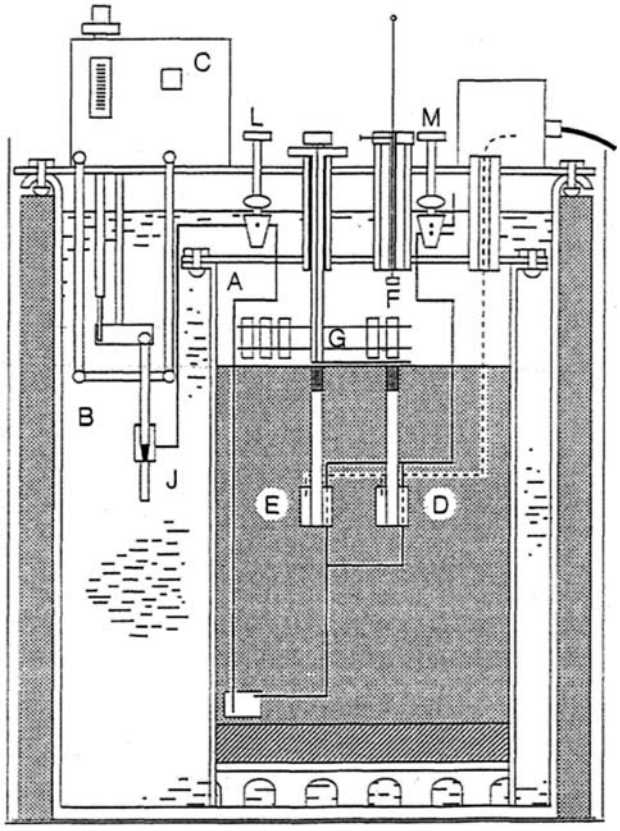

Figure 2. A sketch of the micro-calorimeter used. The calorimeter chamber, A, is submerged in a water bath, B, which is temperature regulated by the thermostat, C. Most of the chamber is filled with polystyrene foam which contains the measuring block, D, and an identical reference block, E. The sample is placed using a magnetic drive, F, on a turntable, G, by which the sample (the cell) is transferred to the measuring block, D, though the magnetic drive after temperature equilibrium is obtained. The two measuring blocks, D and E, are temperature equalized by a water circulatory system consisting of a water injecting pump J and the valves L and M. The valves may be switched so that the tubing system will be filled by air for heat insulation when the apparatus is in measuring mode.

3. Literature Survey

Before the results are presented and discussed a brief summary of the literature is given. Peled and Yamin[4] have put forward a model in which the Li-anode in $SOCl_2$ is always covered by a LiCl-layer. Its minimum thickness on freshly immersed Li is 2–4 nm. The spontaneous formation of LiCl crystals on Li_2O-covered Li was observed after 0.5 min at which time their sizes were about 50 nm. These crystals grew with time, and after 24 h the entire Li surface was covered by a layer of crystals of sizes between 100 nm and 500 nm. This layer acts as a SEI. During storage three things happen, (1) the SEI thickness increases, (2) some of the SEI crystals grow preferentially until they are an order of magnitude or more larger than the SEI thickness, and (3) cracks are formed in the SEI. Using a galvanostatic pulse method and the parallel plate capacitor equation for thickness calculations, a minimum thickness of the SEI which was found to be about 30 nm after 1 day, growing to about 60 nm during the next 2–3 days and levelling off at about 100nm after a month.

Later Peled[2] added to this picture a second type of passivating film consisting of the compact SEI on top of which a thick, mechanically strong, low porosity secondary layer develops.

Independently, Moshtev, Geronov and Puresheva[6] presented a similar model (based on similar measurements and calculations) with a thin (15–50 nm) primary compact LiCl film, and on top of this, a thick (1,000–2,000 nm) porous secondary film. The electrical response is described as originating from the primary film only.

Holleck and Brady[7] also studied freshly exposed Li in $LiAlCl_4/SOCl_2$ by means of galvanostatic pulses. The interpretations were made using the parallel plate capacitor equation as a first approximation. They proposed a film model consisting of three regions. Region I forms rapidly (in less than 1 h). It has a thickness of 20–40 nm. It

appears to have significant imperfection and some microporosity along the grain boundaries. On top of this is the Region II film, which is more ordered and more compact. It grows to 20–60 nm within 20 h. Region III is porous and coarsely crystalline. It is formed by dissolution and recrystallization of the region II film. The paper concludes that the porous film is not detectable by the galvanostatic pulses.

Boyd[25] examined the LiCl film by SEM. He found that the film is composed of two layers: A thin layer of small crystals of 2000–5000 nm size (about 10 x bigger than found by Peled and Yamin[4]) on top of the Li surface and a thicker layer of large crystals on top of them. The thickness of the total layer after 14 days was about 11,000 nm with large crystals about 20,000 nm high. Boyd also looked carefully for a thinner dense film with expected thickness in the range around 70 nm (the thickness found by the galvanostatic pulses), but did not find any. The resolution of his SEM was quote: »several hundred angstroms«.

Chenebault, Vallin, Thevenin and Wiart[12] also performed SEM studies and found the thickness of the LiCl film to be about 80,000 nm after 1 month in A-catholyte. The layer thickness and morphology was affected by various additives. No evidence of a thin compact primary layer was observed. The resolution of the SEM was not stated.

By means of impedance spectroscopy several investigators showed that the capacitance was always frequency dependent.[8,9,13,24,26,27,28] For frequencies in the range of 10–20 kHz, thicknesses in the range of 50–300 nm after 1 day of storage were obtained using the parallel plate capacitor equation.[8,9,26] Selected data from the literature about LiCl-layers on Li in $SOCl_2$-based catholytes are given in Table 2.

Based on a number of SEM studies[1,4,12,25,26] the porosity of the secondary layer is estimated to be no more than a few percent, say max 5% and more probably around 1%. This makes it very difficult to accept that it should not contribute to the electrical response. It should at least block off a lot of surface area of the primary film. Thus, a real discrepancy between the SEM and the electrical parallel-plate-capacitor-model derived thicknesses is seen. Chenebault et al.[13] have discussed and tried to solve this discrepancy by assuming the existence of few narrow cracks going to the very Li-metal surfaces, and it is discussed to which extent the Li-metal is covered by reaction products if at all covered. (It is, however, beyond doubt that the Li is completely covered by LiCl as it is inconceivable that an overvoltage of 3.68 V (the potential of the $SOCl_2$ versus Li) could be sustained without immediate reaction). They conclude themselves that the model works only in very special cases.

Gaberscek, Jamnik and Pejovnik have addressed this problem in a series of papers.[24,16,15,29,30,31,32] It was pointed out that a position dependent resistivity associated with the space charge region might explain the constant phase element (CPE) type of impedance response observed. Further, a model in which the impedance response did not originate from the bulk LiCl at all but only the interface including the space charge region was discussed. A main problem in this model is that it requires a much higher ionic conductivity than the usually found, and in their later paper[32] measurements of the Li^+-conductivity of LiCl grown on Li in $SOCl_2$ (but measured after removing the catholyte) confirmed the usually found low values, i.e. the impedance response originates in fact to a large extent from the bulk of the layer. A pure interface-response model also has difficulties in explaining the reported sensitivity of the impedance to small mechanical impacts.[26]

Table 2. Selected literature data describing the properties of the passivating LiCl layer on Li in $SOCl_2$-based catholytes grown at room temperature. The thicknesses obtained by electrochemical means (impedance spectroscopy or galvanostatic pulses) are compared to results from physical methods SEM, or for one group radioactive Cl-36 (marked with *). The ELCHEM-thicknesses were calculated using the parallel plate capacitor equation. The values marked ** were measured at 25 °C on a film grown at 50 °C after removal of the $SOCl_2$.

Passivation time, days	Thickness, μm SEM	Thickness, μm ELCHEM	Resist., kΩcm^2	K_{LiCl}, nS/cm	Ref. no.
30	50				1
1	0.1–0.5	0.30	0.05	20	4
30	1–5	.01	1	8	4
1	1–2	0.015–0.05	0.25	8–25	6
1		0.04–0.1	1–8	1–5	7
10		0.08	30	0.03, 1.6	9
1	2				25
14	11				25
10	1–2*	0.05	0.07	100	11
30	80		0.9		12
360	~10	0.6	50	6	28
14		80**	1.510^3 **	0.2**	32

4. Results and Discussion

4. 1. Impedance Spectroscopy Data

Fig. 3 shows examples of impedance plots for Li-electrodes in A-, B- and SO_2-catholyte, respectively, all measured 1 day after manufacturing. (The experimental details are given in the Figure caption and in Table 1).

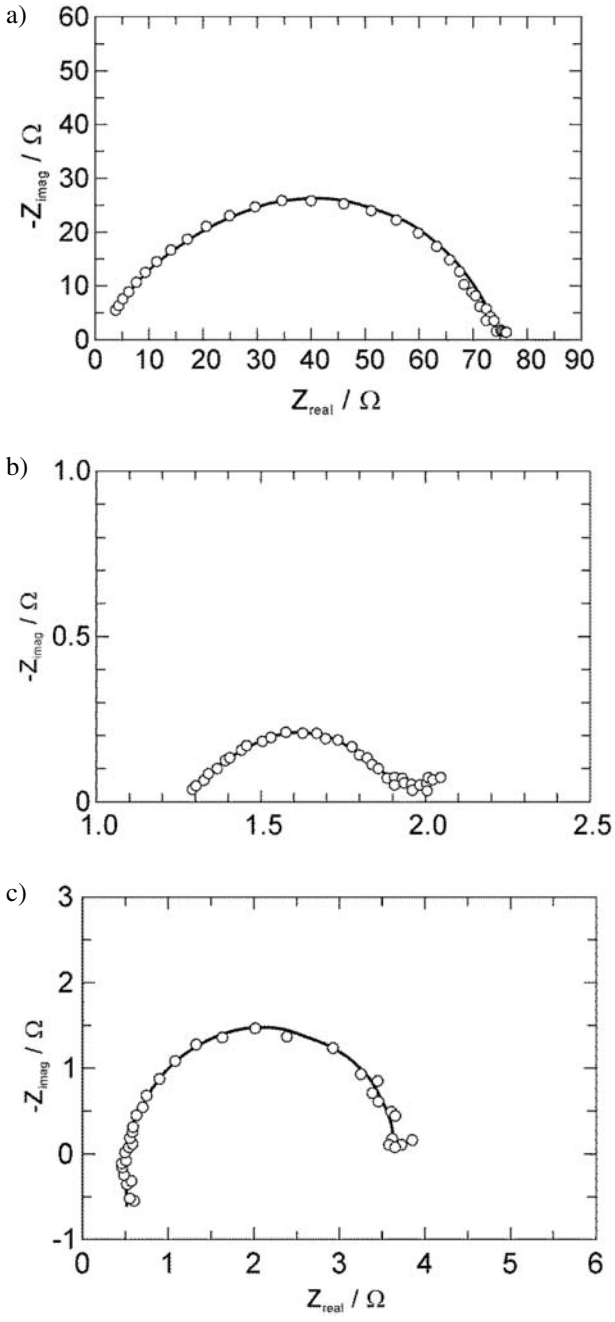

Figure 3. Examples of Impedance spectra measured 1 day after exposure of the Li to the catholyte. a) A-catholyte – cell G40A, b) B-catholyte – cell G24B, and c) SO_2-catholyte – cell SO21. Exposed Li area is 25 cm^2 in all three cases. For further details, see Table 1 and the text.

When the passivation of say 10 different cells has been monitored over some period by the measurement of say 100 impedance spectra containing each typically 75 data-sets consisting of a frequency, a real part and an imaginary part of the impedance then a huge amount of data is at hand. Therefore, there is a great need to reduce this amount in way so that it can be surveyed, and so that it still contains the significant physical information. In an attempt to do this, the impedance measurements have been fitted to two nominally different (but actually kind of redundant, see below) equivalent circuits using the nonlinear least squares fit program written by Boukamp[22]:

Circuit #1: L1 R2 (Q3 R4) (C5 R6) and

Circuit #2: L1 R2 (Q3 (R4 (C5 R6)))

using Boukamp's notation. L denotes inductance, R resistance, C capacitance and Q constant phase angle element (CPE). Often the response of an extra CPE, Q7, is visible at the low frequencies (below 1Hz). The circuits are visualized in Fig. 4. Q is used as the symbol of the CPE.

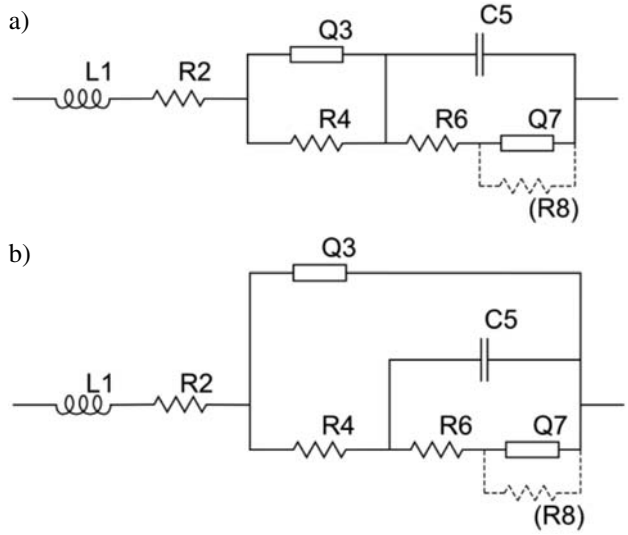

Figure 4. The equivalent circuit used for fitting the impedance spectra. a) circuit #1, b) circuit #2.

It takes two numbers, B and n, to describe the admittance, Y_{CPE}, of a CPE:

$$Y_{CPE} = B \cdot (2 \cdot \pi \cdot f)^n \cdot (\cos(\pi \cdot n/2) + j \cdot \sin(\pi \cdot n/2)) \quad (1)$$

where $j^2 = -1$, and f is the frequency. n is a dimensionless number between 0 and 1, and B must have the dimension Ss^n because the unit of admittance is Siemens (S) and of frequency is s^{-1}. For further details, see e.g. the paper of Boukamp[22] and the book of MacDonald[23]. A short way of writing (1) is:

$$Y_{CPE} = B(j \cdot 2 \cdot \pi \cdot f)^n \quad (1a)$$

In general, there is no reason to believe that such simple equivalent circuits should reflect the real structure of a passivating film on a metal, but, as the fits are fair, it is believed that the values of the equivalent circuit components will contain the essential physical information about the layer and to some extent the measurement set-up. Thus, L1 is inductance originating from leads and equipment, and R2 is serial resistance which for the main part is associated with the lead and the contact to the Li-electrode and for a small part originates from the resistance in the catholyte between the working and the reference electrode. The other quantities, Q3, R4, C5, R6, and Q7 are all believed to be associated with the SEI and/or the SEI interfaces to the Li and the catholyte.

Q7 is mainly of importance in the frequency range below 1 Hz, and the impedances at the low frequencies are not measured with sufficient accuracy to allow a detailed analysis. Q7 was included in several of the fits in order to improve the accuracy of determination of the other parameters. As the Li-anodes are not blocking electrodes, a resistance, R8, must be there in parallel with Q7, but attempts to use it in the fitting did not give meaningful results, and so it was left out. The high capacitance values in the range of mF/cm^2 associated with Q7 have been observed by other workers.[15] It seems that these »supercapacitor«-values are associated with an electrochemical oxidation/reduction of species inside the LiCl-layer close to the Li-metal surface.

The two equivalent circuits used may give exactly the same impedance response if suitable different R, C, B and n values are selected for the two circuits, i.e. it is impossible to distinguish between them by means of fitting a single impedance spectrum. Both were tested because one of the different sets of resulting values may be more probable than the other seen in the light of other available information.

In most measurements the contributions to the impedance diagram from Q3-R4 and C5-R6 overlap. This has earlier been interpreted as a single depressed semi-circle[10,24], and it should be noted that in many cases it is unclear whether the addition of C5 and R6 gives a better fit or not. In some cases it certainly gives a better fit, and so these two equivalent circuits were tested with the hope that some further understanding would be revealed.

Table 3 gives the circuit #1 parameter values per unit area for selected storage times of the cells in Table 1. Table 4 gives the corresponding values of circuit #2 or values obtained using parts of #2. In several cases only a part of #2 was used in order to check if it gave a significant difference for the values derived from the main part of the impedance curve. In cases where C5, R6 and Q7 are omitted there are no differences between #1 and #2.

Figs. 5 and 6 show values of R4, R6, C3 and C5 as a function of time for the anode of cell G40A using circuit #1 and G24B using circuit #2, respectively. In the case of cells with A-catholyte like G40A, the circuits #1 and #2 do not result in much difference in the parameters, whereas for cells with the acid B-type catholyte quite much lower n3-values are obtained by using #1 than by using #2. As n-values lower than 0.5 are difficult to understand

Table 3. Examples of data derived from fitting the impedance spectra to equivalent circiut #1.

Cell	Time days	B3 Ss^{n3}/cm^2	n3	C3 $\mu F/cm^2$	R4 Ωcm^2	C5 $\mu F/cm^2$	R6 Ωcm^2
G40A	1	5.3e-7	0.83	0.12	1680	.17	150
	9	5.4e-7	0.76	0.07	4240	2.22	189
3201	1	6.3e-7	0.81	0.11	1310	137	23
	3	4.2e-7	0.82	0.08	2170	22.6	122
G24B	1	4.0e-4	0.48	0.89	14	23.2	6
	8	1.6e-4	0.43	0.07	24	18.9	4
SO21	1	4.94-5	1.00	48.6	4	14.3	74
	10	2.7e-4	0.75	36.6	13	24.0	38
3303	1	5.2e-5	0.80	9.88	28	56.9	8
	8	2.1e-4	0.61	7.14	28	27.8	16
602	1	4.8e-7	0.92	0.22	364	2.22	120
	6	4.1e-7	0.96	0.29	926	0.19	246
607	1	1.6e-5	0.61	0.42	287	0.37	289
	6	1.7e-6	0.86	0.49	425	0.14	144
610	1	8.8e-7	0.91	0.40	285	0.27	68
	6	1.94-6	0.75	0.18	502	0.45	292
614	1	3.9e-6	1.00	3.88	76	0.39	188
	6	3.0e-6	1.00	3.01	236	3.52	192
618	1	1.7e-6	1.00	1.66	162	0.79	61
	6	6.0e-7	1.00	0.60	310	10.25	101
2REG	1	1.6e-5	0.60	1.25	187	395.	152
	8	1.9e-6	0.70	0.11	960	277.	257

Table 4. Examples of data derived from fitting the impedance spectra to equivalent circiut #2 or parts of it.

Cell	Time days	B3 Ss^{n3}/cm^2	n3	C3 $\mu F/cm^2$	R4 Ωcm^2	C5 $\mu F/cm^2$	R6 Ωcm^2
Ge0A	1	5.2e-7	0.80	0.09	1673	1.15	163
	9	5.4e-7	0.76	0.07	4240	2.22	189
3201	1	6.2e-7	0.81	0.11	1286		
	3	4.0e-7	0.82	0.08	487		
G24B	1	4.8e-5	0.71	0.89	10	12.8	6.3
	8	5.7e-4	0.57	0.25	17.8	12.2	5
SO21	1	1.1e-5	1.00	11.2	49.3	12.8	29.5
	10	1.9e-5	0.95	18.9	18	8.7	32.5
3303	1	3.6e-5	0.83	9	36.5		
	8	7.0e-5	0.73	7.7	44.9		
602	1	3.0e-7	1.00	0.30	480		
	6	5.1e-7	0.87	0.16	1139		
607	1	1.1e-6	0.81	1.12	558		
	6	4.5e-6	0.72	0.37	389	0.08	181
610	1	2.6e-7	0.95	1.30	378	0.12	61
	6	8.3e-7	0.81	0.12	298	0.02	658
614	1	3.8e-7	1.00	0.38	231		
	6	4.3e-6	1.00	0.43	371		
618	1	2.0e-6	0.89	0.72	205		
	6	5.6e-6	1.00	0.56	343		
2REG	1	2.7e-6	0.80	0.33	187		
	8	1.7e-6	0.73	0.13	699		

in the context of a physical layer, circuit #2 was used to generate the data shown in for Fig. 6.

The rather irregular course of C5 in Fig. 5 is often seen and is believed to be associated with cracking of the LiCl film. It should also be noted that odd impedance spectra resulting in odd parameter values are occasionally observed like in the case of G24B after 0.5 day (see Fig. 6, the point with the question mark). The cause may be associated with the variance of the impedance with time which will occur during cracking and the early stage of crack healing. If a major cracking happens during the measurement of an impedance spectrum, it may be recognized as a discontinuity in the spectrum whereas the early stages of crack healing are very difficult to identify with certainty and only question marks can be put up.

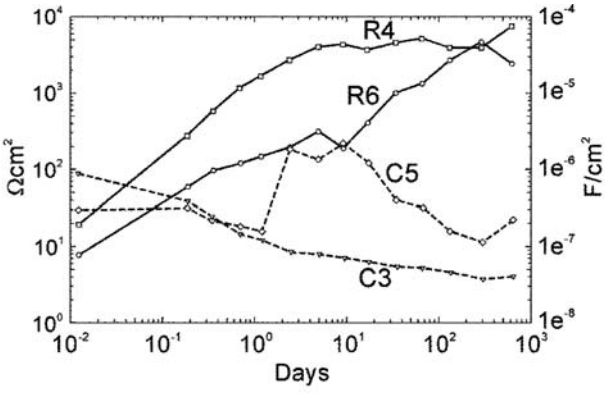

Figure 5. The impedance spectra parameters obtained using circuit #1 as a function of time for cell G40A. C3 was calculated using eq.(8). The values are given in area specific units.

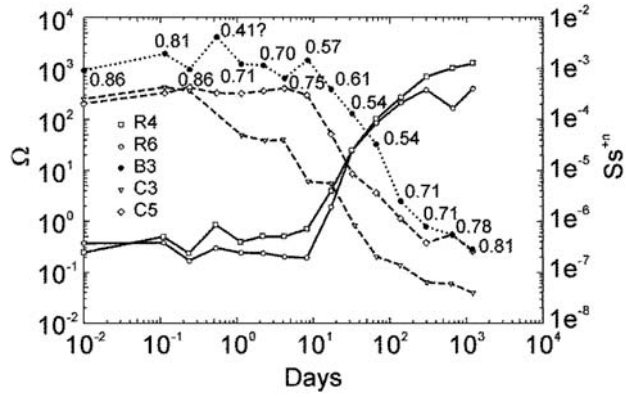

Figure 6. The impedance spectra parameters obtained using circuit #2 as a function of time for cell G24B. Values are given for the full cell area of 25cm². The figures at the B3 curve are the associated n3-values.

4. 2. The Test and Failure of the Parallel-plate-capacitor-model

A way of improving or disproving a model is to try and use it as far as possible, analyse the outcome and then maybe modify the model. Therefore, in this section the impedance data will be treated using the parallel-plate-ca-

pacitor-model in spite of the disagreement reported in section 3. As it will be seen it helps in understanding where and how the model fails and the ionic conductivities derived prove to be fair approximations anyway.

4. 2. 1. Assignment of Circuit Components and Data Treatment

As apparent from section 3 it is widely agreed that the outer part of the LiCl layer on Li in $SOCl_2$ contains porosity and is uneven. Furthermore, a CPE is often associated with porous structures[33] and/or very uneven (fractal) surfaces.[34] On this background, Q3 is interpreted as reflecting (together with R4) the secondary layer. R4 is assumed to be the DC ionic resistance through this layer.

It is of general interest to know the size of the capacitance, C3, associated with Q3, especially as it constitutes a dominant part of the frequency response, and it is believed to be of practical importance to the cell performance. For any given frequency, f, the equivalent capacitance is given by

$$C3(f) = B3 \cdot (2 \cdot \pi \cdot f)^{n-1} \sin(n \cdot \pi/2) \quad (2)$$

The main use of C3 in this subsection is for calculation of the »effective« thickness of the layer to which it is associated. From equation (2) this may seem meaningless as one can get any result from 0 towards infinity depending on the frequencies chosen. The given interpretation, however, puts limits on which frequencies are physically meaningful, i.e. it makes no sense if they are above the range where R4 is fully short circuited (say, $|B3 \cdot (j \cdot 2 \cdot \pi \cdot f)^{n3}|^{-1} << 0.01 \cdot R4$), or below the very low frequencies where $|B3 \cdot (j \cdot 2 \cdot \pi \cdot f)^{n3}|^{-1} >> R4$. It seems also clear that it is not possible to give an unambiguous thickness value for a very uneven porous layer. (It may be like describing the height of a mountain chain like the Alps by a single number). So, it might be argued that by selecting the top point of the Q3-R4-arc, an »electrical average« thickness is obtained, and from a performance point of view this may appear relevant. And, as this comes close to what has been done in many other impedance studies of Li-anodes in $SOCl_2$, this frequency will be used for calculating C3 and a thickness value. This will not be a constant frequency and it cannot usually be picked directly from the frequencies used for the measurements. Thus, this frequency (also called the peak frequency) has to be calculated from the values of the equivalent circuit fitted to the measured data. This was done by the following procedure where the coordinates (a_0,b_0) and (a_{peak},b_{peak}) refer to the centre and the upper most point, respectively, of the depressed semi-circle in a Nyquist diagram:

$$a_{peak} = R2 + R4/2 \quad (3)$$

$$b_0 = R4/(2 \cdot \tan(n3 \cdot \pi/2)) \quad (4)$$

$$b_{peak} = b_0 + R4/(2 \cdot \sin(n3 \cdot \pi/2)) \quad (5)$$

From this the imaginary part of the admittance at the peak,, is found:

$$Y''_{peak} = b_{peak}/((a_{peak}\text{-}R2)^2 + (b_{peak})^2) \quad (6)$$

and the frequency of the peak is given by:

$$f_{peak} = ([Y''_{peak}, /(B3 \cdot \sin(n3 \cdot \pi/2))]^{-n3})/(2 \cdot \pi) \quad (7)$$

$$C3 = Y''_{peak}/(2 \cdot \pi \cdot f_{peak}) \quad (8)$$

Having assigned Q3-R4 to the secondary layer, the only possibilities seen for C5-R6 are that they are associated with either the primary LiCl-layer, or the interfaces of the SEI to Li and/or the catholyte, or both.

Assuming that the Li surface roughness factor is 1, the thicknesses, L_{LiCl}, can be calculated (assuming a parallel plate capacitor):

$$L_{LiCl} = \varepsilon_r \cdot \varepsilon_0/C \quad (9)$$

where the permittivity of vacuum $\varepsilon_0 = 8.84 * 10^{-14}$ F/cm and the relative permittivity of LiCl is $\varepsilon_r = 10.62$.[35] Further, assuming that the distribution and paths of the current lines are independent of frequency, it is possible to calculate the specific ionic conductivity of the layer:

$$K_{LiCl} = \varepsilon_r \cdot \varepsilon_0/(R \cdot C) \quad (10)$$

We are aware that this is an approximation and we do not know the uncertainty. It is, however, believed to give at least a fair estimation of the specific ionic conductivity of the layer, and it is the best approximation that we know.

4. 2. 2. Consequences of the Assignments and Problems Encountered

Two main problems arise as a consequence of the above data treatment. The one may have a solution, but the other has not.

1) The high capacitance problem

Assuming that all C5-R6 belong to the primary layer, ionic conductivities and layer thicknesses can be calculated using the formulas above. Results are shown in Table 5. It shows very low thicknesses in many cases, and the ionic conductivities are unexpectedly low, sometimes lower than the conductivity of the secondary layer (Table 6) which is supposed to be of purer LiCl than the primary layer.[26]

Table 5. Result derived from C5-R6, the »primary layer«, using circuit #1. The ratio of free to blocked area in the »secondary layer«, $a_{p,sec}$, is calculated assuming that the »true« thickness of the »primary layer« is 3 nm. See text for details.

Cell	Time days	K_{LiCl} S/cm	Thickness nm	$a_{p,sec}$
G40A	1	3.8e-8	56	0.05
	9	2.2e-9	4.2	0.71
3201	1	3.0e-10	0.07	>1
	3	3.4e-10	0.41	>1
G24B	1	7.1e-9	0.40	>1
	8	1.2e-8	0.50	>1
SO21	1	8.8e-10	0.65	>1
	10	1.0e-9	0.39	>1
3303/SO2	1	2.0e-9	0.17	>1
	8	2.0e-9	0.34	>1
602	1	3.5e-9	4.2	0.71
	6	2.0e-8	49	0.06
607	1	8.8e-9	25	0.12
	6	4.8e-8	69	0.04
610	1	5.0e-8	34	0.09
	6	7.1e-9	21	0.14
614	1	1.3e-8	24	0.12
	6	1.4e-9	2.67	>1
618	1	2.0e-8	12	0.25
	6	9.1e-10	0.9	>1
2REG	1	1.6e-11	0.02	>1
	8	1.3e-11	0.03	>1

The problem of very thin layers is especially pronounced in the SO_2-catholytes. It simply does not make physical sense when the calculated sum of the primary and secondary layer thicknesses is below 1 nm and the electron tunnelling distance is about the double or more. Thus, these extremely high values of C5 (and C3) need some other explanation.

Then it seems natural to associate C5-R6 with the Li/LiCl and /or the LiCl/$SOCl_2$ interfaces. However, just ascribing C5 to compact Helmholtz layers is also problematic. The unit length of the LiCl-grid is 0.514 nm, corresponding to a distance between the planes (1,1,1) of 0.324 nm and a distance between similar atoms of 0.363nm. According to equation (9) a thickness of 0.324 nm corresponds to a capacity of C_c = C5 = 29 μF/cm² of the compact Helmholtz layer. According to the Stern model and derived models it may look as if this value will also be the maximum possible total capacity when the compact Helmholtz layer capacity is added to the diffuse (space charge) layer capacity, C_d, by the formula $1/C5 = 1/C_c + 1/C_d$ (see textbook, e.g. Fried[36]). This is, however, not believed to be generally valid. It is only valid if the charge transfer resistance $R_t \rightarrow \infty$. If the time constants (i.e. the capacitances and the resistance) of the processes in question are enough different, then the parallel C_c-R_t will appear to be in series connection with the parallel C_d-R_d (R_d is the ionic resistance of the space charge region).

Then the next question is if such high capacitances at all can be associated with the space charge regions. Therefore, as an example, 200 μF/cm² is inserted into the equation of differential capacity of the diffuse double layer

$$C5 = z \cdot F \cdot (\mathrm{sqr}\{2 \cdot \varepsilon_r \cdot \varepsilon_0 \cdot c/(R \cdot T)\} \cdot \cosh (E \cdot z \cdot F/(2 \cdot R \cdot T)) \quad (11)$$

or

$$E = (2 \cdot R \cdot T/(z \cdot F)) \cdot \mathrm{arccosh}(C5/(z \cdot F \cdot \mathrm{sqr}\{2 \cdot \varepsilon_r \cdot \varepsilon_0 \cdot c/(R \cdot T)\})) \quad (12)$$

which, using a guess of concentration of vacancies of c = 10^{-7} mol/cm³, gives a zeta-potential of 0.32V. An independent measurement of the zeta-potential would be commendable, but the electrode cannot be polarized much without changing its properties (morphology). Taking into account that the total voltage across the LiCl SEI is 3.68V, the 0.32V seems reasonable.

It is recognized that the uncertainty on the determination of the capacitance is rather high, but anyway the size of the capacitances, which must be accounted for in certain cases, seems to be of the order of 100μF/cm² or more.

From the data and this discussion it is concluded that the impedance responses of the Li-anode covered with very thin films reflect more than the simple properties of thickness and ion conductivity of the film. Also the interface including the space charge regions are reflected.

2) The secondary layer blocking effect problem

When the secondary layer is not 100% dense, only a maximum value of its LiCl ionic conductivity, $K_{LiCl,max}$, can be calculated using eq.(10) because part of the conduction will take place through catholyte-filled cracks and pores, i.e.

$$K_{LiCl,max} = \varepsilon_r \cdot \varepsilon_0/(R4 \cdot C3) \quad (10a)$$

If a pore area ratio is defined as

$$a_{p,sec} = A_{p,sec}/A_{total} \quad (13)$$

where A_{total} is the nominal electrode area, and $A_{p,sec}$ is the effective area available for conduction of ions through the full distance of the LiCl-thickness through catholyte-filled pores, and the conduction paths are assumed to have geometries with parallel walls perpendicular to the Li-surface, then it can be shown that

$$a_{p,sec} < K_{LiCl,max}/K_{lyte} \quad (14)$$

where K_{lyte} is the specific conductivity of the catholyte.

As already mentioned Q3-R4 is assigned to the secondary layer. This means that an apparent thickness, L_{LiCl}, the maximum conductivity, and the maximum pore

area ratio can be calculated from eqs. (9), (10a) and (14), respectively. Table 6 shows the data for the anodes given in Table 1 using the data of Table 3.

Table 6. Results derived from Q3-R4, the »secondary layer«, using circuit #1. The ratio of free to blocked area in the »secondary layer«, $a_{p,sec}$, is calculated using eq.(14).

Cell	Time Days	L_{LiCl} nm	$K_{LiCl,max}$ S/cm	$a_{p,sec}$
G40A	1	76.	4.6e-9	2.3e-7
	9	132.	3.1e-9	1.6e-7
3201	1	82.	6.2e-9	3.1e-7
	3	113.	5.2e-9	2.6e-7
G24B	1	10.6	7.7e-8	3.9e-6
	8	139.	5.7e-7	2.9e-5
SO21	1	0.2	4.8e-9	4.8e-8
	10	0.3	2.0e-9	2.0e-8
3303	1	1.0	3.4e-9	3.4e-8
	8	1.3	4.7e-9	4.7e-8
602	1	44.	1.2e-8	6.0e-7
	6	32.	3.5e-9	1.7e-7
607	1	22.	7.8e-9	3.9e-7
	6	19.	4.5e-9	2.3e-7
610	1	23.	8.2e-9	4.1e-7
	6	52.	1.0e-8	5.2e-7
614	1	2.4	3.2e-9	1.6e-7
	6	3.1	1.3e-9	6.6e-8
	1	5.7	3.5e-9	1.8e-7
	6	16.	5.1e-9	2.5e-7
2REG	1	37.	2.0e-8	9.9e-7
	8	86.	8.9e-9	4.5e-7

From Table 6 it is clear that a model similar to Chenebault's[13] implies rather dense secondary layers with a crack cross section area fraction (pore area ratios) generally below 10^{-6}. Holleck and Brady[7] reported similar densities, but concluded that the porous layer could not be seen by electrochemical means. This conclusion cannot be correct, and when analysing the data of Tables 5 and 6 in detail, this is recognised as a more general problem. In order to illustrate this, it is assumed for a moment that the primary layer thickness, $L_{pri,}$ has a fixed value of 3nm. The fact that it is covered by a secondary layer is expected to block off the surface resulting in a lower measured capacitance, i.e. if no correction is made for this, a too big L_{pri} would be obtained by using eq.(9). In fact a pore area ratio, $a_{p,sec}$ as defined above, might be calculated as the ratio between the true and the apparent thickness of the primary layer:

$$a_{p,sec} = L_{pri,true}/L_{pri,app} = L_{pri,true} \cdot C5/(\varepsilon_r \cdot \varepsilon_0) \qquad (15)$$

If $L_{pri,true}$ = 3 nm, all cases (see Table 5) will give $a_{p,sec} > 0.04$ in sharp contrast to the numbers derived from C3-R4 (Table 6). Many values will even become above 1 because of the space charge capacitances resulting in apparent thicknesses lower than 3 nm. The $a_{p,sec}$-values of Table 5 infer that the secondary layer is at least quite porous, above 4%, and in most cases non-existent, which is in clear disagreement with SEM-observations. The problem is not eased by proposing that C5-R6 belongs to the interface because the actual active area would be $(a_{p,sec})^{-1}$ times the nominal area. This means that if the $a_{p,sec}$-values of Table 6 are believed to be correct then the real capacitances per cm^2 should be more than 10^6 times bigger than the »measured« C5-values of Tables 3 and 4 resulting in values up into the range of hundred Farads per cm^2. This is of course not possible.

In other words, the parallel-plate-capacitor-model has failed and so has in fact the associated concept of a simple double-layer model. And a model with more layers will not help. Another kind of model is needed.

4. 3. Alternative Model Considerations

A complete physical model should explain all aspects of the impedance spectra. Unfortunately, the low frequency data available are too uncertain to allow a further analysis, and so the considerations are restricted to the high frequency (>50Hz) part of the impedance spectrum which, due to the sizes of the involved capacitance, is supposed to reflect the bulk of the layer. The model should then explain the CPE parameters, B3 and n3, and the resistance, R4.

The most direct way of obtaining insight in the structure is by microscopic observations. The SEM studies show that at least the outer parts of the passivating layer are formed by LiCl precipitation from the liquid catholyte because very smooth crystal growth facets are

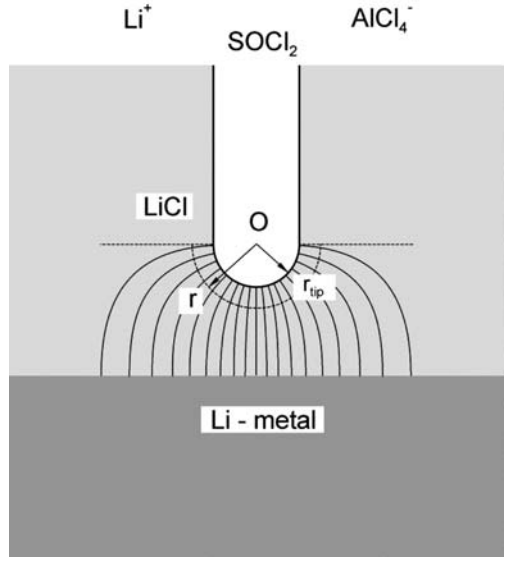

Figure 7. Illustration of the concept behind eqs. (16)–(19). With rotational symmetry it shows a cylindrical hole ending in a semisphere, eqs. (16)–(17a). If a cross-section through a crack is imagined then it shows a crack with a tip of semi-cylindrical shape.

seen. This in turn means that differences in radius of curvature of the various surface parts of the LiCl layer, are delivering the driving force for the dissolution and re-precipitation of the LiCl, and thus, it seems probable that catholyte-filled tunnels along the LiCl crystal corners will be left in the layer and possibly some types of crystal faces may have difficulties in growing totally together. It is inherent in such a model that the dimensions of the tunnels in the inner part (towards the Li) of the LiCl have to be in the nanometer range because the crystals themselves are in the range of 100 – 1000 nm size.

Thus, the focus is put on the resistive and capacitive responses of narrow deep holes and cracks as sketched in Fig. 7. If rotational geometry is imagined in Fig. 7 then it is a hole with a half-sphere tip with radius, r_{tip}. If crack geometry is envisaged, Fig. 7 shows a crack width of $2*r_{tip}$, and the crack tip is a half-cylinder with radius r_{tip}. Making the approximation that the current does not flow »backwards«, the following formulas (see textbook, e.g. Lehner[37]) may be used for calculating the capacitances and resistances as a function of distance, r, from the hole or crack tip center:

For holes:

$$R(r) = (1/(2 \cdot \pi \cdot K_{LiCl})) \cdot (1/r_{tip} - 1/r) \quad (16)$$

$$R_{max} = 1/(2 \cdot \pi \cdot K_{LiCl} \cdot r_{tip}) \quad (16a)$$

$$C(r) = 2 \cdot \pi \cdot \varepsilon_r \cdot \varepsilon_0 \cdot (r_{tip} r/(r-r_{tip})) \quad (17)$$

$$C_{min} = 2 \cdot \pi \cdot \varepsilon_r \cdot \varepsilon_0 \cdot r_{tip} \quad (17a)$$

For cracks per unit length:

$$R(r) = (1/(\pi K_{LiCl}))\ln(r/r_{tip}) \quad (18)$$

$$C(r) = \pi \cdot \varepsilon_r \cdot \varepsilon_0 \cdot (\ln(r/r_{tip})^{-1} \quad (19)$$

Here, it should be noted that irrespective of geometry the conductivity is given by eq. (10) which is also obtained by solving eqs. (16) and (17) as well as eqs. (18) and (19) with respect to the conductivity, K_{LiCl}.

If the distance from the crack tip to the Li-metal is used for r in eqs.(16–19) a better approximation is believed to be at hand compared to just assuming a »parallel plate« compact layer. Naturally, if the distance from the tip to the Li is less than or equal to the tip dimensions the parallel plate may locally be a better approximation. Furthermore, it should be noted that eqs.(18) and (19) will also be good approximations for calculating the resistance and capacitance of the LiCl on the Li-side of tunnels parallel to the Li-surface of the type shown in Fig. 8a.

Table 7 gives some examples of the resistances through narrow tunnels and cracks which are filled with catholyte and of the resistance in the LiCl next to the tips of the holes and cracks tips/tunnels parallel to the Li, respectively. It is seen that even though the resistance in catholyte-filled cracks may be relatively small, the resistance of the LiCl at the tip is large also in cases where the distance to the Li is only 10 nm. Tunnels perpendicular to the Li do not lower the layer resistance much unless there are an enormous number of them.

This information may be applied to a typical Li-anode passivated in A-catholyte for about a week. The »SEM-thickness« is about 10,000nm (10μm as an average figure, but it is very non-uniform). The measured values are: R4 = 7 kOhm cm^2, B3 = 2.6 · 10^{-7} S $s^{-0.8}cm^{-2}$, n3 = 0.8

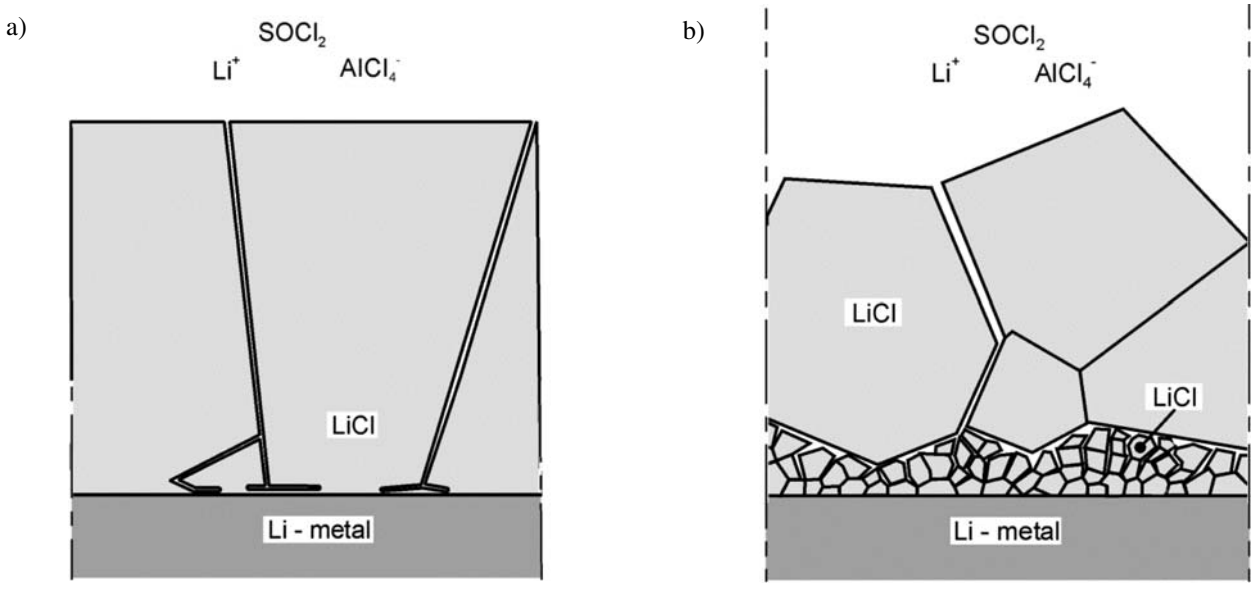

Figure 8. Sketches of possible structures of the LiCl passivating layer. The »simple crack« model (a) cannot explain the CPE type of impedance response. A very branched crack and tunnel system (b) seems necessary, and the small grains towards the Li-metal with bigger grains on top reflects the structures observed by SEM.[25]

Table 7. Examples of calculated resistance through catholyte filled tunnels and cracks filled with 1.8M $LiAlCl_4/SOCl_2$-catholyte and of the solid LiCl at hole and crack tips.

Through tunnels Tunnel	Resistance
dia., nm	Ω/μm
10	6.4e8
100	6.4e6
1000	6.4e4
Through 1 cm long cracks	
Crack width, nm	Resistance Ω/μm depth
10	5e3
100	500
1000	50

In the LiCl at hole tips. Resistance, R in Ω, and capacitance, C in F.
Hole diameter, nm

	10		100		1000	
Distance, nm	R	C	R	C	R	C
10	8.16e13	4.42e-18	4.00e14	7.37e-19	4.00e13	7.37e-19
100	1.16e14	3.05e-18	8.16e12	4.424-17	4.00e14	7.37e-18
1000	1.21e14	2.96e-18	1.16e13	3.10e-17	8.16e11	4.42e-16
Max/min	1.22e14	2.95e-18	1.22e13	2.95e-17	1.22e12	2.95e-16

In the LiCl at 1 cm long crack tips. Resistance, R in Ω, and capacitance, C in F.
Crack width, nm

	10		100		1000	
Distance, nm	R	C	R	C	R	C
10	1.35e8	2.68e-12	3.85e7	9.39e-12	3.85e6	9.39e-11
100	3.73e8	9.69e-12	1.35e8	2.68e-12	3.85e7	9.39e-12
1000	6.49e8	5.56e-13	3.73e8	9.67e-13	1.35e8	2.68e-12

and the layer capacitance C3 = 51 $nFcm^{-2}$. This implies a $K_{LiCl} = 2.6*10^{-9}$ S/cm. The resistance of the layer (10 μm thick) without cracks is then calculated to be 380 kOhm cm^2 and the capacitance 0.94 nF/cm^2. This is a real set of data for A-catholyte, selected to compare well with data reported by others.[1,7,8,9,11,12,27,28] From this, it is possible to make a rough estimate of which lengths of tunnels parallel to the Li are necessary in order to explain the actually observed resistance. If it is assumed that the tunnel diameter is 10 nm and the distance to the Li surface is 100 nm then it is found that the length necessary to give a resistance of 7000 Ωcm^2 is $5*10^4$ cm/cm^2. This may be compared to the calculated length of LiCl grain boundaries in one plane parallel to the Li. If the grains are assumed having forms of hexagons of 500 nm size and having all centres in this plane, the grain boundary length is $3.3*10^4$ cm/cm^2. In reality the grains are irregularly shaped and have a size distribution. The grain corners consti-

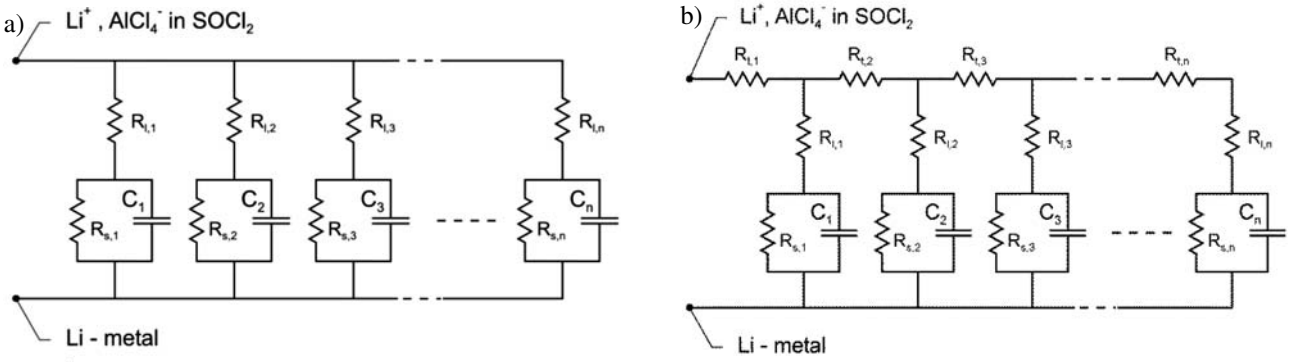

Figure 9. Electrical circuits tested as models of the LiCl layer. Fig. 9a is simulating the »simple crack« model of Fig. 8a, and 9b is another »ladder« type of circuit. which may respond as a CPA over certain frequency ranges dependent on the actual values of resistances and capacitances. Even higher degrees of branching are necessary in order to simulate the observed CPE behaviour pointing to a much branched crack and tunnel system.

tute a three dimensional network which will result in a much longer grain corner length in the layer of small crystals near the Li-surface than obtained by the above simple calculation. Altogether, it seems to suggest that some, not vanishing, fraction of the grain corners and faces are open and catholyte-filled. This indicates a structure of the passivating layer similar to the type shown in Fig. 8b.

Another indication of a much branched crack and tunnel system, as illustrated in Fig. 8b, may be revealed. For this purpose, the simpler structure of Fig. 8a is considered. It might be thought that in a structure with only a few cracks and tunnels, a relative simple equivalent circuit of the kind shown in Fig. 9a could possibly model the LiCl film response, i.e. Q3-R4. This was tried. Naturally, when many circuit parameters are available, it is easy to find values which result in a flat arc of the same size as a measured one. It is, however, only possible to achieve something near to a CPE behaviour if the $R_{s,i} \cdot C_i$ is varying significantly. The consequence of this is that either should the LiCl electrical permittivity or the conductivity decrease towards the Li-surface. None of the possibilities is thought to be likely. The LiCl relative permittivity is about 10 only, so it is not conceivable that it should decrease to 1. The decrease of the conductivity would be in agreement with the position dependent conductivity idea,[16] but this would imply a CPE behaviour in all cases and from Table 3 and 4 it is seen that this is not the case. Finally, the circuit of Fig. 9a does not give a real constant phase angle, i.e. not a real CPE, while the impedance response of the LiCl layer is a real CPE over 4 frequency decades from about 10Hz to 10 kHz. In order to obtain a CPE type of behaviour some kind of branching of resistance and capacitance in a ladder type of circuit is necessary, see e.g. the book of McDonald.[23] Such a kind of circuit is shown in Fig. 9b, and here a depression of the impedance spectrum arc may be achieved over some range of frequency. An analysis show that in this case only an n3-value of 0.5 may be obtained, and in order to get an n3 = 0.75, one more level of branching is necessary, with e.g. Fig 9b type of circuits in the side of the "ladder" and pure capacitances as »steps« (if Fig. 9b is imagined to be a ladder, $R_{t,1}$, $R_{t,2}$ .....$R_{t,n}$ is constituting the one side of the ladder and $R_{e,1} + R_{s,1} + C_1$ is step no. 1 etc.) The experimental results show that n3 may vary with time and with catholyte composition, and in fact may vary from anode to anode under nominally identical conditions. This points to a picture with a variable high degree of branching like Fig. 8b, which shows a tunnel system on the boundaries of the small grains next to the Li. This system is covered by big massive (not porous) 10–20 μm grains with a few big cracks between them, reflecting the situation in an A-catholyte after some days. Such a system is believed to form a transmission line network which may account for the varying n3 values seen.

This qualitative model provides an explanation of the course of passivation of Li in the B-catholyte shown in Fig.6. During the period from the first measurement after 15 min (0.01 day) to about 10 h almost no change in values are seen. This is due to little re-precipitation of LiCl from the acid B-catholyte which can absorb a significant amount of LiCl which it is also able to release again depending on the chemical activity of the LiCl, i.e the radius of curvature locally on the single LiCl crystals. After this period n3 and C3 start to decrease. This is understood as a result of large crystals being nucleated on the top of the small crystals which were already formed before the first measurement. During the first days after this nucleation, the resistances are not affected very much, but after about 12 days the large crystals start to grow together resulting in a drastic increase of the LiCl-film resistance. After about 200 days this increase levels off meaning that now the large crystal layer are as dense as it possibly will become at all. About the inflection point of the resistance curve n3 reach a value close to 0.5. This is taken as the point where the »transmission lines« consisting of the tunnels beneath the big crystals are longest just before a large part of the tunnel system is blocked off by the big crystals growing into each other.

4. 4. Micro-calorimetry and LiCl Electronic Conductivity

Table 8 shows selected values from the microcalorimetric measurements. The typical range of heat production during the first days is 1 – 10 μW/cm².

For the Li-$SOCl_2$-system having a well defined EMF = 3.68 V, the measured power (heat) can be directly transformed to self discharge current. A source of error is thermal decomposition of thionyl chloride. Frank[38] states

Table 8. Microcalorimetry result and the derived electronic conductivities. $K_{ele} = \varepsilon_r \cdot \varepsilon_0/(R_{ele} \cdot C)$. Min K_{ele} is obtained using C3 data from Table 2, and max K_{ele} is found from $C_{total} = (1/C3 + 1/C5)^{-1}$ using Table 2 data. $R_{ele} = EMF^2/W$, where W is the power density

Cell	Time Days	Power density μW/cm²	EMF V	R_{ele} MΩcm²	Min. K_{ele} S/cm	Max. K_{ele} S/cm
3201	1	1.05	3.68	12.9	6.4e-13	1.1e-12
	3	4.82	3.68	2.8	4.0e-12	4.3e-12
3303	1	9.85	3.3	1.1	8.6e-14	9.3e-14
	8	1.93	3.3	5.6	2.4e-14	3.1e-14
2REG	1	11.88	3.68	1.1	3.4e-12	3.4e-14
	8	3.00	3.68	4.5	1.9e-12	1.9e-14

a rate of EXP(–0.12–1605/T))%/day, which at 25 °C gives 1,5%/year, the same level as normal self-discharge rates for aged lithium batteries.

The reaction 4 $SOCl_2$ = 2 SO_2 + S_2Cl_2 + 3 Cl_2 gives a total enthalpy of –33.3 kcal/mol. For a cell having 19 g thionyl chloride, it is equivalent to a 10 μW/cell, which normally is much less than the measured effects, but higher rates of decomposition, for example from catalytic reactions, cannot be excluded.

At large self-discharge rates or intentional loads (in the range 5–100 kΩ) there should be a further correction for the entropy-related heat production[39–41]). The Gibbs-Helmholtz equation may be written as

$$nFE = -Q + nFT(dE/dT) \quad (20)$$

where n = number of electrons, F = Faradays constant, E = EMF, –Q = heat production, T = temperature. The equation may be rewritten as

$$-QI/(nF) = E^2/R - T(E/R)(dE/dT) \quad (21)$$

where R = the discharge resistance. The first term contains the total heat flow including self-discharge and loss from polarization, the next term the heat production in the discharge resistor, and the last term includes Q_E, the heat production of the electrode reaction.

dE/dT is found to be –0.00029 V/K for unused cells (having A-catholyte), –0.00039 V/K for 1% discharged and –0.00044 V/K for 50% discharged cells. As an example, the correction Q_E is 33 μW (i.e. 1 μW/cm²Li) at a 10 kΩ discharge and 3 μW at a 100 kΩ discharge. The correction is insignificant at normal self-discharge currents.

So, the electron conductivities given in Table 8 were calculated from the microcalorimetric measurements assuming that the electron conductivity, K_{ele}, is the only factor that limits the self-discharge:

$$K_{ele} = \varepsilon_r \cdot \varepsilon_0/(R_{ele} \cdot C) \quad (10b)$$

and

$$R_{ele} = EMF^2/W \quad (22)$$

where W is the heat power density. The C3 values of Table 3 were used. The results are in fair agrement with the values in the range $3 \cdot 10^{-12}$ –$5 \cdot 10^{-13}$ S/cm reported in a previous paper [8] in which the electronic conductivity of the LiCl was estimated from the growth rate in certain stages where the parabolic law was followed.

4. 5. General Discussion

The analyses presented show that impedance spectroscopy cannot be used as a reliable method of measuring the thicknesses of the LiCl-films using the parallel plate capacitor formulas, but the formulas derived for the conductivities are believed to be good approximations because the geometric parameters cancel when the equations are solved with respect to conductivity. There is some uncertainty on the values because of the uncertainty on the capacitances derived from CPEs. The magnitude of this »uncertainty« is dependent on the n3-value. If the previous mentioned example (R4 = 7 kΩ cm^2, B3 = $2.6*10^{-7}$ S $s^{-0.8}cm^{-2}$, n3 = 0.8) is used, application of the peak frequency of 423 Hz gives K_{LiCl} = 2.6 nS/cm and the frequency of 20 kHz (where the high frequency part of the impedance curve approaches the real axis) gives 5.8 nS/cm. This difference does not reflect any kind of measurement uncertainty. It is because of model limitations, i.e. the »probing« includes different amounts of the LiCl layer with different fractions of catholyte filled porosities according to the model presented above, but as the model is not quantitative the different amounts are not known. It means that the LiCl-conductivities are upper limits, and it points out that the lower frequencies should give the most reliable values, but then there is the problem that at low frequencies other sources than the LiCl layer contribute to the impedance spectrum. The Q3-R4- peak frequency still seems to be no bad choice for the calculation of the conductivities.

A point of general concern in the context of lithium batteries with liquid catholytes is the delayed voltage phenomenon and the explanation of it. The present work does not provide any proof of one or the other interpretation of the delayed voltage effect, but the mechanical cracking and peeling hypothesis is in a way the consequence of the model of Figs. 8b, i.e. the concentrated currents at the crack tips will cause local heating and stress build-up which in turn cause the cracking and peeling. This hypothesis is also in agreement with the observation that a high current for a short time is more effective than a low current for a longer time in effectively removing the delayed voltage. More importantly, it is also in agreement with SEM micrographs of the surfaces (Dey[42]) showing large extents of cracks, and the fact that delayed voltage experiments are difficult to reproduce. On the other hand the hypothesis does apparently not agree with Delnick,[9] who finds that during transition, noise is not superimposed on the discharge current. However, each crack only contributes to a minor part of the total current, so that current versus time curves may appear smooth especially when the super-capacitances at the very low frequencies (Q7) are recalled. Such capacitances will certainly be able to smoothen quite big jumps in the Faradaic current.

Further, the presented model (and data) implies that the dissolution and redisposition of LiCl by the catholyte is responsible for the build-up of such a relatively bulky microporous passivating layer. If the LiCl stayed where it was originally formed, the formation of the big blocking crystals would not take place.

5. Conclusions

Analysis of experimental observations has resulted in a qualitative model of the passivating LiCl layer formed on Li in liquid cathodes. The layer is 100% dense towards the Li-metal but otherwise microporous due to numerous tunnels and crevices along the LiCl grain boundaries and some cracks. The structure is changing with time and conditions. It is shown that the double LiCl-layer model and the parallel plate capacitor equation are not applicable, and thus a meaningful thickness of the passivating layer cannot be derived from impedance spectroscopy. In spite of this, impedance spectroscopy is a valuable tool for monitoring and studying the Li passivation as it gives, in a non-destructive manner, a reliable layer resistance and an approximate specific ionic resistivity. Using parallel measurements of impedance spectroscopy and microcalorimetry provide approximate values of the LiCl specific electronic conductivity. This is of special importance for the general description of the layer since the electronic conductivity is controlling the LiCl formation and the self-discharge of the Li-battery.

6. Acknowledgments

This work has been supported by the Danish Energy Agency under the EFP projects 1443/88-2 and 1443/89-2. The discussions with Drs. Miran Gaberscek and Janez Jamnik, The National Institute of Chemistry, Ljubljana, Slovenia, were very helpful. The principal author (MBM) is especially grateful to the Director of The National Institute of Chemistry, Ljubljana, Slovenia, Prof. Stane Pejovnik, for the invitation to stay as a guest scientist for 3 months at The Institute during 1996, 20 years ago. The authors are grateful to Dr. Karin Vels Hansen, DTU Energy, for help during the finishing of the manuscript.

7. References

1. A. N. Dey, *Thin Solid Films* **1977**, *43*, 131. http://dx.doi.org/10.1016/0040-6090(77)90383-2
2. E. Peled, in »Lithium Batteries«, J. P. Gabano, Ed.,Chap. 3, Academic Press, Inc., 1983.
3. E. Peled, H. Straze, *J. Electrochem. Soc.* **1977**, *124*, 1030. http://dx.doi.org/10.1149/1.2133474
4. E. Peled, H. Yamin, Proc. 28th. *Power Sources Symp.* **1978**, p. 237.
5. R. G. Keil, T. N. Wittberg, J.R. Hoenigman, C. R. McDonald, Proc. 29th. *Power Sources Symp.*, **1980**, p.132.
6. R. V. Moshtev, Y. Geronov, B. Puesheva, *J. Electrochem. Soc.* **1981**, *128*, 1851. http://dx.doi.org/10.1149/1.2127750
7. G. L. Holleck, K. D. Brady, in Proc. Symp. on Lithium Batteries, 1984, PV 84-1, 48, The Electrochemical Soc., Pennington, NJ.
8. M. Mogensen, in Proc. 6th Risø Internat. Symp. on Metallurgy and Materials Science, 1985, p. 233. This reference is also found as an appendix to Ref. 10.
9. F. M. Delnick, in Proc. Symp. on Primary and Secondary Ambient Temperature Lithium Batteries, 1988, PV 88-6, 212, The electrochemical Soc., Pennington, NJ.
10. M. Mogensen, Report Risø-M-2619, 1987.
11. V. E. Kazarinov, V. S. Bagotzky, *J. Power Sources*, **1987**, *20*, 259. http://dx.doi.org/10.1016/0378-7753(87)80121-0
12. P. Chenebault, D. Vallin, J. Thevenin, R. Wiart, *J. Applied Electrochem.* **1988**, *18*, 625. http://dx.doi.org/10.1007/BF01022261
13. P. Chenebault, D. Vallin, J. Thevenin, R. Wiart, *J. Applied Electrochem.* **1989**, *19*, 413. http://dx.doi.org/10.1007/BF01015245
14. F. M. Delnick, *J. Power Sources* **1989**, *26*, 129. http://dx.doi.org/10.1016/0378-7753(89)80022-9
15. J. Jamnik, M. Gaberscek, A. Meden, S. Pejovnik, *J. Electrochem. Soc.* **1991**, *138*, 1582. http://dx.doi.org/10.1149/1.2085837
16. J. Jamnik, M. Gaberscek, S. Pejovnik, *Electrochimica Acta* **1990**, *35*, 423. http://dx.doi.org/10.1016/0013-4686(90)87022-T
17. R. R. Dogonadze, A. M. Kuznetsof, J. Ulstrup, *Electrochimica Acta* **1977**, *22*, 967. http://dx.doi.org/10.1016/0013-4686(77)85008-1
18. M. Mogensen, in Proc. 9th. Scandinavian Corrosion Congress, Vol. 2, 1983, p. 699. This reference is also found as an appendix to Ref. 10.
19. R. W. Berg, H. A. Hjuler, A. P. L. Søndergaard, N. J. Bjerrum, *J. Electrochem. Soc.* **1989**, *136*, 323. http://dx.doi.org/10.1149/1.2096629
20. J. P. Gabano, G. Gelin, in Proc. 12th International Power Sources Symposium, (J. Thompson, ed.), Academic Press, 1981, paper no. 1.
21. A. N. Dey, H. C. Kuo, D. Foster, C. Schlaikjer, M. Kallianidis, Proc. Int. Power Sources Symp. 1986, 32, 176.
22. B. A. Boukamp, *Solid State Ionics* **1986**, *20*, 31. http://dx.doi.org/10.1016/0167-2738(86)90031-7
23. J. R. Macdonald, Impedance spectroscopy (New York, John Wiley & Sons 1987.
24. M. Gaberscek, J. Jamnik, S. Pejovnik, *J. Power Sources* **1989**, *25*, 123. http://dx.doi.org/10.1016/0378-7753(89)85004-9
25. J. W. Boyd, *J. Electrochem. Soc.* **1987**, *134*, 18. http://dx.doi.org/10.1149/1.2100402
26. M. Mogensen, in Proc. Symp. on Primary and Secondary Ambient Temperature Lithium Batteries 1988, PV88-6, 229, The electrochemical Soc., Pennington, NJ.
27. M. Mogensen, *J. Power Sources* **1985**, *14*, 123. http://dx.doi.org/10.1016/0378-7753(85)88021-6
28. M. Mogensen, *J. Power Sources* **1987**, *20*, 53. http://dx.doi.org/10.1016/0378-7753(87)80090-3
29. M. Gaberscek, J. Jamnik, S. Pejovnik, *J. Power Sources*

1993, *43–44*, 391.
http://dx.doi.org/10.1016/0378-7753(93)80179-S
30. M. Gaberscek, J. Jamnik, S. Pejovnik, *J. Electrochem. Soc.* **1993**, *140*, 308.
http://dx.doi.org/10.1149/1.2221043
31. M. Kovac, M. Gaberscek, S. Pejovnik, *J. Appl. Electrochem.* **1994**, *24*, 1001.
http://dx.doi.org/10.1007/BF00241191
32. D. Kek, M. Gaberscek, S. Pejovnik, *J. Electrochem. Soc.* **1996**, *143*, 1690.
http://dx.doi.org/10.1149/1.1836701
33. A. Lasia, in *Modern Aspects of Electrochemistry*, *Number 43*, M. Schlesinger (Ed.), pp 67 – 138, DOI: 10.1007/978-0-387-49582-8_3, Springer, New York, 2009.
http://dx.doi.org/10.1007/978-0-387-49582-8_3
34. A. Le Mehaute, in Proc. 6th Risø Internat. Symp. on Metalurgy and Materials Science, 1985, p. 25.
35. Gmelin Handbuch der Anorganischen Chemie, System-Nummer 20, (Weinheim 1960) 333.
36. I. Fried, The chemistry of electrode processes, London, Academic Press, 1973.
37. G. Lehner, Elektromagnetische Feldttheorie für Ingenieure und Physiker, 2. Auflage, Springer-Verlag, Berlin, 1994.
38. H. A. Frank, The Electrochemical Society Pittsburgh Meeting 1978, abstract 58.
39. E. S. Takeuchi, Meyer S. M., Holmes C. F., *J. Electrochem. Soc.* **1990**, *137*, 1665.
http://dx.doi.org/10.1149/1.2086768
40. Kalu E. E., White R. E., Darcy E. C., *J. Electrochem. Soc.* **1992**, *139*, 2378. http://dx.doi.org/10.1149/1.2221234
41. Kalu E. E., White R. E., Darcy E. C., *J. Electrochem. Soc.* **1992**, *139*, 2755. http://dx.doi.org/10.1149/1.2068975
42. A. N. Dey, *Electrochimica Acta* **1976**, *21*, 377.
http://dx.doi.org/10.1016/0013-4686(76)85029-3

Povzetek

Opisana je študija impedančne spektroskopije litijevih anod pasiviranih z LiCl v različnih tekočih katodah (katolitih) na osnovi $LiAlCl_4$ v $SOCl_2$ oz. SO_2. Impedančni spektri so bili razloženi s pomočjo dveh ekvivalentnih vezij z uporabo metode nelinearnih namanjših kvadratov. S pomočjo te metode smo ekstrahirali informacije o ionski prevodnosti in strukturi plasti. Predlagali smo nov fizikalni opis, ki razlaga parametre vezja. Domneva se, da plasti LiCl vsebujejo veliko število ozkih tunelov in razpok, ki so napolnjene s tekočim katolitom. Razložili smo tudi, zakaj omenjeni tuneli nastajajo. Na specifičnem primeru smo pokazali, da so tuneli povezani z večino mej med zrni kristalinične plasti LiCl v bližini Li površine ter, da so nujno potrebni pri razlagi impedančnega odziva. Hitrost nastanka plasti LiCl, je omejena z elektronsko prevodnostjo le-te. Podatki mikrokalorimetrije so skupaj z impedančnimi spektri služili za določevanje elektronske prevodnosti plasti LiCl.